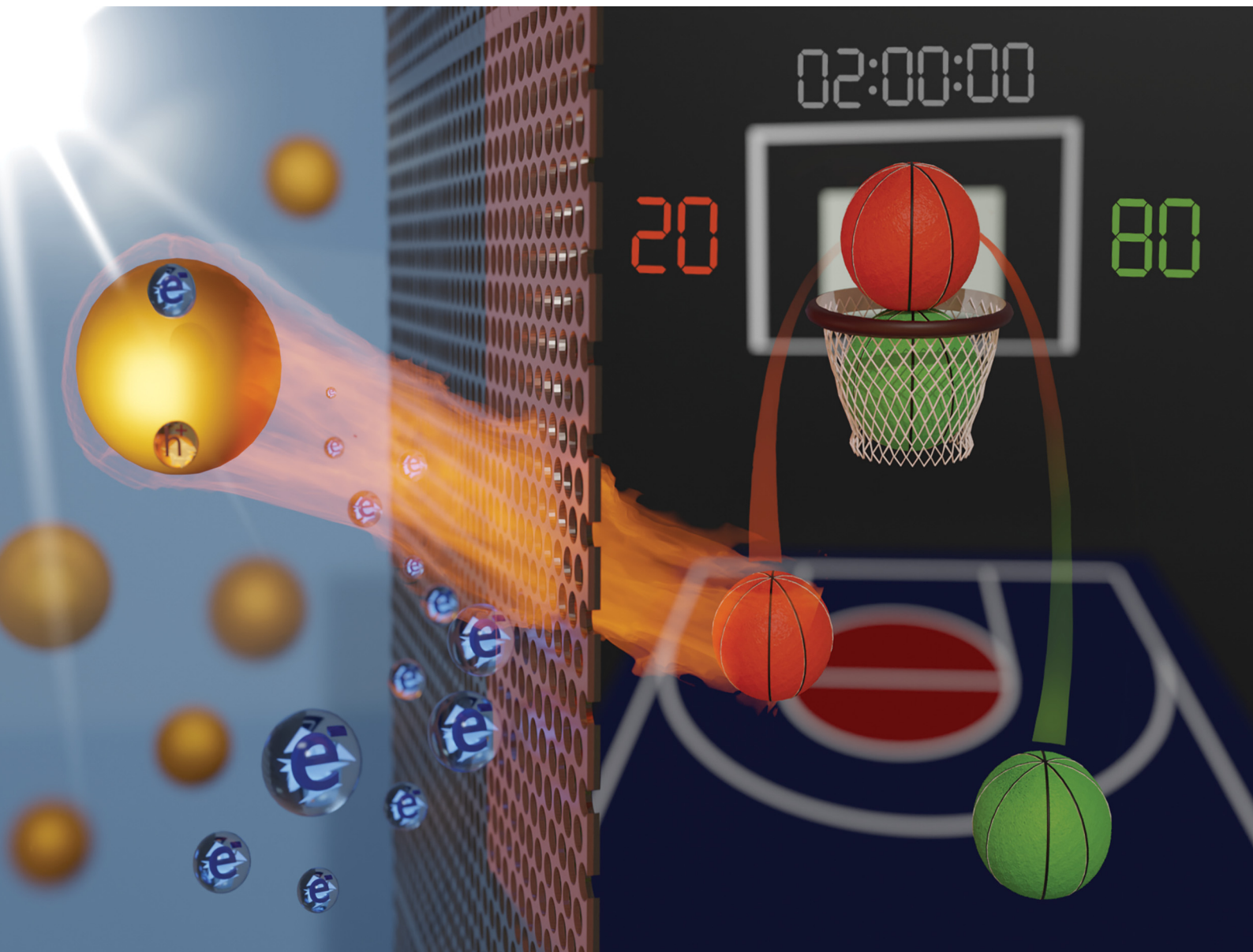


# ChemComm

Chemical Communications

rsc.li/chemcomm



ISSN 1359-7345



# Plasmon enabled Claisen rearrangement with sunlight†

 Radha Krishna Kashyap,<sup>ib</sup> Shreya Tyagi and Pramod P. Pillai<sup>ib\*</sup>

 Cite this: *Chem. Commun.*, 2023, 59, 13293

 Received 31st August 2023,  
 Accepted 9th October 2023

DOI: 10.1039/d3cc04278b

rsc.li/chemcomm

Plasmonic-heat generated from the solar irradiation of gold nanoparticles is used as the thermal energy source for the Claisen rearrangement of allyl phenyl ether to 2-allylphenol, which is conventionally performed with electrical heating at 250 °C. The use of a closed reactor enables the physical separation of the reactants from the source of plasmonic-heat, thereby preventing the interference of the hot-charge carriers in the plasmon-driven Claisen rearrangement. In this way, the sole effect of plasmonic-heat in driving a high temperature organic transformation is demonstrated. Our study reveals the prospects of plasmonic nanostructures in conducting energy intensive chemical synthesis in a sustainable fashion.

The visible-light absorbing power of plasmonic nanoparticles (NPs) is exceptionally high ( $10^8$ – $10^{10}$  M<sup>-1</sup> cm<sup>-1</sup>) because of their unique excitation pathway based on surface plasmon resonance.<sup>1</sup> A photoexcited NP can dissipate its excess energy through radiative and non-radiative pathways: *ca.* ~5% and ~95%, respectively, for NPs with size <25 nm.<sup>2</sup> The main outcomes of the radiative relaxation pathway are scattering and emission; whereas, hot-charge carrier generation and heat-dissipation are the main outcomes of the non-radiative relaxation pathway.<sup>3</sup> Both hot-charge carrier generation and heat-dissipation can bring out important chemical and physical transformations, which constitute the areas of plasmonic photocatalysis<sup>4</sup> and thermoplasmonics,<sup>5</sup> respectively. The majority of the photoexcitation energy in plasmonic NPs is dissipated in the form of heat because of the fast charge recombination dynamics associated with non-radiative relaxation processes (100 fs–10 ps; Landau damping, electron–electron, electron–phonon, and phonon–phonon scattering).<sup>3</sup> In effect, the amount of heat dissipated by a photoexcited NP is huge because of the involvement of unique excitation and relaxation pathways (photothermal

conversion efficiency is >90%).<sup>6</sup> This heat dissipated from a photoexcited NP is termed as plasmonic-heat, which has found use in various photothermal applications including therapy,<sup>7</sup> drug delivery,<sup>8</sup> solar-vapor generation,<sup>9</sup> azeotropic separation,<sup>10</sup> and material synthesis.<sup>11</sup>

Recent studies have proved the suitability of plasmonic-heat in synthetic organic chemistry as well, with the aim of achieving sustainability in chemical synthesis.<sup>12</sup> The idea here is to use the plasmonic-heat as the thermal energy source, instead of the conventional electrical heating, for performing high temperature organic reactions. However, it has been challenging to deconvolute the contribution of hot-charge carriers in a plasmonic-heat driven organic reaction, as both these outcomes are part of the same nonradiative decay process.<sup>13</sup> In this work, the use of a proper reactor system enabled us to prevent the interference of the hot-charge carriers and study the sole effect of plasmonic-heat in high temperature organic reaction (Scheme 1). This was achieved by



**Scheme 1** Schematic representation of plasmonic-heat driven Claisen rearrangement of allyl phenyl ether to 2-allylphenol. The photoexcitation of plasmonic AuNPs leads to a series of nonradiative processes: Landau damping, electron–electron ( $e^-e^-$ ), electron–phonon ( $e^-ph$ ), and finally heating-up the local environment via the phonon–phonon ( $ph-ph$ ) interactions. This heat dissipated from the plasmonic AuNPs was used as the thermal energy source for the Claisen rearrangement.

Department of Chemistry, Indian Institute of Science Education and Research (IISER) Pune, Dr. Homi Bhabha Road, Pashan, Pune-411 008, India.

E-mail: pramod.pillai@iiserpune.ac.in

† Electronic supplementary information (ESI) available: Experimental information, synthesis, additional characterization, and Movie S1. See DOI: <https://doi.org/10.1039/d3cc04278b>

designing a thermodynamically closed reactor system, wherein the reaction mixture was physically separated from the plasmonic NPs (heating source). This will enable the exchange of energy (here, plasmonic-heat), whereas the exchange of matter (here, hot charge carriers) will be prevented. Our choice of the high temperature organic reaction was the thermally driven [3,3] sigmatropic Claisen rearrangement of allyl phenyl ether to 2-allylphenol, which is conventionally performed at 250 °C using electrical heating.<sup>14</sup> Also, Claisen rearrangement is one of the commonly practiced reactions in synthetic organic chemistry to form carbon-carbon bonds, further justifying the importance and choice of the reaction in the present study.<sup>15</sup> The plasmonic-heat dissipated from gold nanoparticles (AuNPs) was used as the thermal energy source for the Claisen rearrangement, which gave an excellent yield of ~80% within 2 h of solar irradiation. Kinetic studies reveal that the rate of the reaction under plasmonic-heating was at least two times higher than the reaction performed with normal electrical heating, which can be attributed to the higher steady-state temperature achieved with plasmonic-heat.

AuNPs were chosen as the plasmonic NP in the present study because of their strong absorption power in visible-light and high photostability under continuous solar irradiation.<sup>1</sup> AuNPs of diameter  $12.0 \pm 0.4$  nm were synthesized using a modified seed-mediated growth method<sup>16</sup> (see Fig. 1 and Fig. S1, S2 in the ESI†). The surface of the AuNPs was functionalised with 11-mercaptoundecanoic acid (MUA) to enhance the colloidal stability of the NPs in the aqueous medium. This enabled the entire photothermal studies with AuNPs from the same batch. The rationale behind selecting ~12 nm AuNPs was based on the knowledge that AuNPs in the size range of 10–24 nm show the highest photothermal conversion efficiency.<sup>17</sup> The surface plasmon band of AuNPs (centred at ~520 nm) has a strong overlap with the solar spectrum, enabling the use of sunlight as the irradiation source (Fig. 1a). Along with testing the suitability of plasmonic-heat in high temperature organic synthesis, our objective was to eliminate the contribution from hot-charge carriers in a plasmon-driven organic reaction. For this, a thin film of plasmonic AuNPs was coated on the surface of aluminium (Al) foil that was wrapped around the glass test



Fig. 1 (a) UV-visible absorption studies show a strong overlap between the surface plasmon band of AuNPs (centred at ~520 nm) and the solar spectrum, confirming the suitability of sunlight as the irradiation source. The solar spectrum was adapted from the ASTM G173-03 AM1.5G reference spectrum with permission. (b) A representative transmission electron microscope (TEM) image of  $12.0 \pm 0.4$  nm AuNPs.

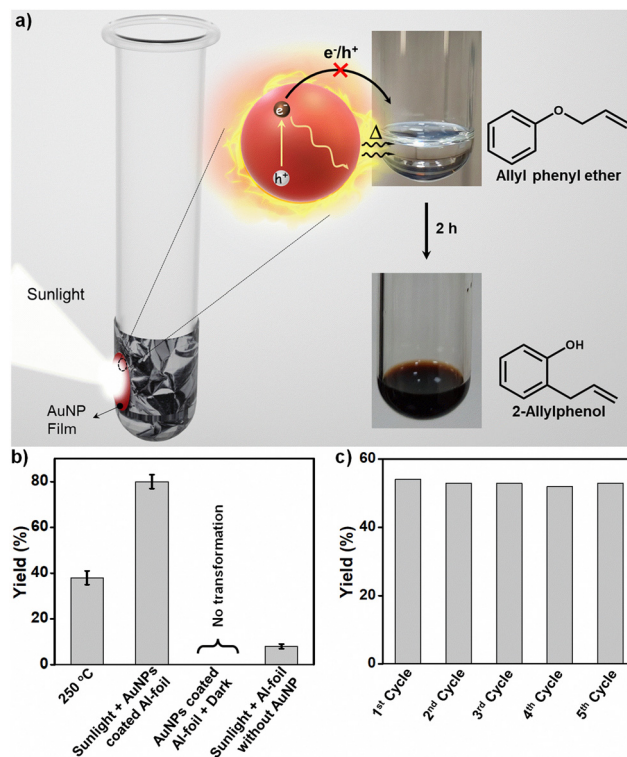


Fig. 2 (a) Schematics of the thermodynamically closed reactor used for the plasmonic-heat driven Claisen rearrangement. The optical photographs of the reaction medium before and after 2 h of solar illumination are shown on the right side. (b) Bar diagram showing the yield obtained under different experimental conditions, which conclusively prove the sole role of plasmonic-heat in driving the Claisen rearrangement. (c) Bar diagram showing the retention of photothermal activity of plasmonic AuNPs for at least five cycles.

tube (here, reactor) (see Fig. 2a and Fig. S3 in the ESI†). The Al-foil interface helped in achieving a stable coating of AuNPs on the test tube. Also, the high thermal conductivity of Al ( $205 \text{ W m}^{-1} \text{ K}^{-1}$ ) ensured the effective transfer of the plasmonic-heat to the reactants inside the glass test tube. The physical separation of the reactants from the plasmonic-heat source (here, AuNPs) prevented the transfer of hot-charge carriers to the reactant. Furthermore, the wrapping of the reactor with Al-foil will block the direct exposure of the reactants to sunlight, thereby overruling the interference of photochemical effects as well. Yet another advantage of the closed reactor is that the reaction mixture will not be contaminated with the plasmonic-heaters. In this way, a simple design of a closed reactor enabled us to study the sole effect of photothermal properties in a plasmon-driven organic reaction.

Claisen rearrangement was selected as the model reaction to study the potential of plasmonic-heat in performing high-temperature organic synthesis. The intramolecular ortho rearrangement of the allylic group in allyl phenyl ether to form 2-allylphenol *via* [3,3] sigmatropic rearrangement is an energy intensive thermal transformation, which is conventionally performed at 250 °C (Fig. 2a). Our idea was to replace the traditional electrical-heat with plasmonic-heat generated from the

solar irradiation of AuNPs. In a typical photothermal experiment, the AuNP coated Al-foil wrapped test tube containing 1 mL of allyl phenyl ether was irradiated with focused sunlight (experimental details are provided in the ESI†). The colourless reactant turned to reddish yellow within 2 h of solar irradiation, indicating the thermal conversion of allyl phenyl ether to 2-allylphenol. The reaction mixture was purified, and the product was characterized using  $^1\text{H-NMR}$  and HRMS studies (Fig. S4 and S5 in the ESI†). All the yields were calculated from the  $^1\text{H-NMR}$  of the reaction mixture using the internal standard method (1,1,2,2-tetrachloroethane was used as the internal standard) (see Fig. S6 and S7 in the ESI† for details of yield calculation). The plasmonic-heat driven Claisen rearrangement resulted in a yield of  $\sim 80\%$  after 2 h of solar irradiation (Fig. 2b and Fig. S8 in the ESI†), which was at least double the yield obtained from normal thermal reaction performed at  $250\text{ }^\circ\text{C}$  under similar experimental conditions (Fig. 2b and Fig. S9 in the ESI†). The enhancement in the yield under solar irradiation can be explained as follows. The amount of energy absorbed by AuNPs upon solar irradiation is exceptionally high ( $\sim 10^8\text{ M}^{-1}\text{ cm}^{-1}$ ), because of the phenomenon of surface plasmon resonance.<sup>1</sup> The photoexcited AuNPs undergo a series of nonradiative relaxation processes (Landau damping, electron–electron, electron–phonon, and phonon–phonon interactions) to eventually dissipate the excess energy in the form of plasmonic-heat.<sup>3</sup> It has been shown that the plasmonic-heat can raise the surface temperature of AuNPs to  $600\text{ }^\circ\text{C}$ ,<sup>18</sup> which will be finally dissipated to the surrounding medium. As a result, the temperature experienced by the surrounding medium close to the plasmonic AuNPs can be as high as  $\sim 500\text{ }^\circ\text{C}$ .<sup>12</sup> In the present study too, a higher steady-state temperature ( $>250\text{ }^\circ\text{C}$ )<sup>9b</sup> could have been experienced by the reactants because of the plasmonic-heat dissipated from the photoexcited AuNPs, leading to an improvement in the product yield under solar irradiation. Control experiments (i) in the dark at room temperature under similar experimental conditions with an AuNP film coated Al-foil wrapped test tube (Fig. 2b and Fig. S10 in the ESI†) and (ii) under sunlight illumination of allyl phenyl ether reactant in an Al-foil wrapped test tube without the AuNP film produced negligible yields (Fig. 2b and Fig. S11 in the ESI†), confirming the necessity of plasmonic-heat in performing the reaction. It is worth mentioning that the Al-foil completely blocks the focused sunlight from entering the test tube (Fig. S12, ESI†), which overrules the possibility of the thermal shielding effect arising from the confinement of light by Al-foil. Movie S1 (ESI†) clearly shows the vigorous boiling, along with a distinct color change to reddish yellow, when the AuNP coated test tube containing allyl phenyl ether reactant (b.p. =  $191.7\text{ }^\circ\text{C}$ ) was irradiated with sunlight. In this particular experiment, the AuNP film was coated inside the glass test tube for the in-situ visualisation of the progress of the reaction (control experiments in the absence of AuNPs fail to show any boiling as well as conversion of the reactant. Details are given in the ESI†). All these control experiments confirm the sole-involvement of plasmonic-heat as the thermal energy source in the Claisen rearrangement of allyl phenyl ether to

2-allylphenol. The plasmonic-heaters based on AuNPs also showed excellent reusability with negligible loss in the photothermal reaction yield for at least five cycles (Fig. 2c and Fig. S13 in the ESI†), which can be attributed to their high photostability under continuous solar irradiation (the time of the reaction was reduced to 90 min to complete multiple cycles under similar solar irradiation power).

Finally, the rate of the Claisen rearrangement under plasmonic- and electrical-heating was compared. The progress of the reaction was monitored by analysing the product yield in aliquots collected at different time intervals (see ESI† for the experimental details). NMR studies revealed a gradual increase in the product yield with time (Fig. 3a and b), for both plasmonic and electrical-heating driven Claisen rearrangement. The NMR signal at  $3.5\text{ ppm}$  corresponding to the product increased with time of heating, accompanied by a decrease in the reactant signal at  $4.55\text{ ppm}$  (Fig. 3c and Fig. S14, S15 in the ESI†). Approximately  $80\%$  product was formed under the plasmonic-heating condition after 2 h of solar irradiation. In contrast, the normal electrical-heating at  $250\text{ }^\circ\text{C}$  required  $\sim 6\text{ h}$  to yield  $\sim 80\%$  product formation (Fig. S15 in the ESI†). The rate of the reaction under plasmonic-heating conditions was at least two times higher than the one under electrical-heating, which confirms that the steady-state temperature achieved with plasmonic-heat is higher than  $250\text{ }^\circ\text{C}$ .

In conclusion, an energy intensive high temperature Claisen rearrangement was performed with an excellent yield of  $\sim 80\%$  using the plasmonic-heat generated from the solar irradiation



Fig. 3 (a) A plot showing the variation in the product yield with respect to time for plasmonic-heat (red) and electrical-heat (blue) driven Claisen rearrangement. (b) The bar diagram showing the corresponding reaction rates. (c) A plot showing the variation in  $^1\text{H-NMR}$  signal with respect to time for plasmonic-heat driven Claisen rearrangement (only the region covering the distinguishable peaks of reactant and product is shown for clarity).

of AuNPs. Control experiments conclusively prove the sole role of plasmonic-heat as the thermal energy source for driving the Claisen rearrangement. The high photostability of AuNPs ensured the constant supply of heat energy for performing the Claisen rearrangement, under continuous and repeated solar irradiations. More importantly, an appropriate design of a closed reactor enabled the physical separation of reactants from the source of the plasmonic-heat generator, which prevented the interference from the hot-charge carriers. In short, our study reveals the potential of plasmonic-heating as an alternative to electrical-heating for high-temperature organic reactions, thereby showcasing a way to achieve sustainability in high-temperature chemical synthesis.

R. K. K. prepared the AuNPs, and conducted and analysed the photothermal organic reactions. S. T. performed the characterization studies and analysed the data. P. P. P. conceived the project, wrote the manuscript with the assistance of all co-authors, and coordinated the research.

The authors acknowledge the financial support from MoE-STARs Grant No. MoE-STARs/STARs2/2023-0195. The authors thank U.S. Department of Energy (DOE)/NREL/ALLIANCE for the ASTM G173-03 AM1.5G reference spectrum. The authors thank Namitha Deepak and Mridul K. Vinod for helping with TOC, scheme preparation and sunlight experiments. R. K. K. thanks CSIR and S. T. thanks UGC for the PhD fellowships.

## Conflicts of interest

There are no conflicts to declare.

## Notes and references

- (a) S. Link and M. A. El-Sayed, *J. Phys. Chem. B*, 1999, **103**, 8410–8426; (b) J. H. Hodak, I. Martini and G. V. Hartland, *J. Phys. Chem. B*, 1998, **102**, 6958–6967; (c) C. F. Bohren, *Am. J. Phys.*, 1983, **51**, 323–327.
- (a) C. Sönnichsen, T. Franzl, T. Wilk, G. von Plessen, J. Feldmann, O. Wilson and P. Mulvaney, *Phys. Rev. Lett.*, 2002, **88**, 077402; (b) A. M. Brown, R. Sundararaman, P. Narang, W. A. I. Goddard and H. A. Atwater, *ACS Nano*, 2016, **10**, 957–966.
- (a) H. Inouye, K. Tanaka, I. Tanahashi and K. Hirao, *Phys. Rev. B: Condens. Matter Mater. Phys.*, 1998, **57**, 11334–11340; (b) S. Link and M. A. El-Sayed, *Annu. Rev. Phys. Chem.*, 2003, **54**, 331–366; (c) M. L. Brongersma, N. J. Halas and P. Nordlander, *Nat. Nanotechnol.*, 2015, **10**, 25–34; (d) C. Boerigter, U. Aslam and S. Linic, *ACS Nano*, 2016, **10**, 6108–6115; (e) V. Jain, R. K. Kashyap and P. P. Pillai, *Adv. Opt. Mater.*, 2022, **10**, 2200463.
- (a) S. Linic, P. Christopher and D. B. Ingram, *Nat. Mater.*, 2011, **10**, 911–921; (b) S. Mukherjee, F. Libisch, N. Large, O. Neumann, L. V. Brown, J. Cheng, J. B. Lassiter, E. A. Carter, P. Nordlander and N. J. Halas, *Nano Lett.*, 2013, **13**, 240–247; (c) S. Roy, S. Roy, A. Rao, G. Devatha and P. P. Pillai, *Chem. Mater.*, 2018, **30**, 8415–8419; (d) S. Roy, V. Jain, R. K. Kashyap, A. Rao and P. P. Pillai, *ACS Catal.*, 2020, **10**, 5522–5528; (e) V. Jain, I. N. Chakraborty, R. B. Raj and P. P. Pillai, *J. Phys. Chem. C*, 2023, **127**, 5153–5161; (f) A. Dhankhar, V. Jain, I. N. Chakraborty and P. P. Pillai, *J. Photochem. Photobiol. A*, 2023, **437**, 114472; (g) J. Kuno, N. Ledos, P.-A. Bouit, T. Kawai, M. Hissler and T. Nakashima, *Chem. Mater.*, 2022, **34**, 9111–9118; (h) R. Verma, R. Tyagi, V. K. Voora and V. Polshettiwar, *ACS Catal.*, 2023, **13**, 7395–7406.
- (a) A. O. Govorov and H. H. Richardson, *Nano Today*, 2007, **2**, 30–38; (b) G. Baffou and R. Quidant, *Laser Photonics Rev.*, 2013, **7**, 171–187; (c) L. Jauffred, A. Samadi, H. Klingberg, P. M. Bendix and L. B. Oddershede, *Chem. Rev.*, 2019, **119**, 8087–8130; (d) M. J. Margeson, Y. E. Monfared and M. Dasog, *ACS Appl. Opt. Mater.*, 2023, **1**, 1004–1011; (e) B. Klemmed, L. V. Besteiro, A. Benad, M. Georgi, Z. Wang, A. Govorov and A. Eychmüller, *Angew. Chem., Int. Ed.*, 2020, **59**, 1696–1702; (f) M. Dhiman, A. Maity, A. Das, R. Belgamwar, B. Chalke, Y. Lee, K. Sim, J.-M. Nam and V. Polshettiwar, *Chem. Sci.*, 2019, **10**, 6594–6603; (g) S. A. Mezzasalma, J. Kruse, S. Merckens, E. Lopez, A. Seifert, R. Morandotti and M. Grzelczak, *Adv. Mater.*, 2023, 2302987; (h) S. Roy, R. K. Kashyap and P. P. Pillai, *J. Phys. Chem. C*, 2023, **127**, 10355–10365.
- (a) H. H. Richardson, M. T. Carlson, P. J. Tandler, P. Hernandez and A. O. Govorov, *Nano Lett.*, 2009, **9**, 1139–1146; (b) H. Breitenborn, J. Dong, R. Piccoli, A. Bruhaes, L. V. Besteiro, A. Skripka, Z. M. Wang, A. O. Govorov, L. Razzari, F. Vetrone, R. Naccache and R. Morandotti, *APL Photonics*, 2019, **4**, 126106.
- (a) L. R. Hirsch, R. J. Stafford, J. A. Bankson, S. R. Sershen, B. Rivera, R. E. Price, J. D. Hazle, N. J. Halas and J. L. West, *Proc. Natl. Acad. Sci. U. S. A.*, 2003, **100**, 13549–13554; (b) X. Huang, I. H. El-Sayed, W. Qian and M. A. El-Sayed, *J. Am. Chem. Soc.*, 2006, **128**, 2115–2120.
- (a) T. Sun, Y. S. Zhang, B. Pang, D. C. Hyun, M. Yang and Y. Xia, *Angew. Chem., Int. Ed.*, 2014, **53**, 12320–12364; (b) M. S. Strozyk, S. Carregal-Romero, M. Henriksen-Lacey, M. Brust and L. M. Liz-Marzán, *Chem. Mater.*, 2017, **29**, 2303–2313.
- (a) O. Neumann, A. S. Urban, J. Day, S. Lal, P. Nordlander and N. J. Halas, *ACS Nano*, 2013, **7**, 42–49; (b) R. K. Kashyap, I. Dwivedi, S. Roy, S. Roy, A. Rao, C. Subramaniam and P. P. Pillai, *Chem. Mater.*, 2022, **34**, 7369–7378.
- O. Neumann, A. D. Neumann, E. Silva, C. Ayala-Orozco, S. Tian, P. Nordlander and N. J. Halas, *Nano Lett.*, 2015, **15**, 7880–7885.
- R. Kamarudheen, G. Kumari and A. Baldi, *Nat. Commun.*, 2020, **11**, 3957.
- (a) C. Fasciani, C. J. B. Alejo, M. Grenier, J. C. Netto-Ferreira and J. C. Scaiano, *Org. Lett.*, 2011, **13**, 204–207; (b) E. N. Van Burns and B. J. Lear, *J. Phys. Chem. C*, 2019, **123**, 14774–14780; (c) J. Qiu and W. D. Wei, *J. Phys. Chem. C*, 2014, **118**, 20735–20749; (d) C. Vázquez-Vázquez, B. Vaz, V. Giannini, M. Pérez-Lorenzo, R. A. Alvarez-Puebla and M. A. Correa-Duarte, *J. Am. Chem. Soc.*, 2013, **135**, 13616–13619.
- L. Zhou, D. F. Swearer, C. Zhang, H. Robotjazi, H. Zhao, L. Henderson, L. Dong, P. Christopher, E. A. Carter, P. Nordlander and N. J. Halas, *Science*, 2018, **362**, 69–72.
- (a) L. Claisen, *Ber. Dtsch. Chem. Ges.*, 1912, **45**, 3157–3166; (b) A. M. Martín Castro, *Chem. Rev.*, 2004, **104**, 2939–3002; (c) X. Han and D. W. Armstrong, *Org. Lett.*, 2005, **7**, 4205–4208.
- M. Hiersemann and U. Nubbemeyer, *The Claisen Rearrangement*, Wiley-VCH, Weinheim, 2007.
- (a) N. R. Jana and X. Peng, *J. Am. Chem. Soc.*, 2003, **125**, 14280–14281; (b) A. Rao, S. Roy, M. Unnikrishnan, S. S. Bhosale, G. Devatha and P. P. Pillai, *Chem. Mater.*, 2016, **28**, 2348–2355.
- R. K. Kashyap, M. J. Parammal and P. P. Pillai, *ChemNanoMat*, 2022, **8**, e202200252.
- C. Wang, O. Ranasingha, S. Natesakhawat, P. R. Ohodnicki, M. Andio, J. P. Lewis and C. Matranga, *Nanoscale*, 2013, **5**, 6968–6974.